

# On ridges and valleys

Juan Serrat, A. López and D. Lloret  
Computer Vision Center & Dept. Informàtica  
Edifici O, Universitat Autònoma de Barcelona  
08193 Cerdanyola, Spain  
e-mail joans@cvc.uab.es

## Abstract

*Ridges and valleys are earth's relief structures. They can have an imaging counterpart provided we model a digital image as a landscape by considering grey level values as height. These two dual entities have received comparatively little attention from the computer vision community with regard to others like edges or corners. In this paper we first propose a taxonomy or classification of the several definitions of ridge and valley lines and review their implementation on discrete images. Then, we illustrate the application of one type of characterization, a creaseness measure, to solve several problems of image registration, where ridge and valley lines are taken as landmarks.*

## 1. Introduction

Common operators in image analysis and computer vision such as the gradient, curvature, laplacian etc. lie on the implicit modeling of images as the discretization of a graphic surface. A particular case within this general model is to think of grey-level images as the sampling of a topographic relief or landscape. This conception gives rise to build new operators or algorithms which approximate, in the discrete, geomorphological entities like ridge and valley lines, watersheds, basins or drainage patterns. Despite an image does not actually represent height measurements in a landscape's array of sites, as would be the case of digital elevation model (DEM) images, those entities can be of great value. Often, they closely correspond to structures of interest for analysis purposes. In general, ridge and valley lines have been applied mostly for 1) computation of medial axes or skeletons, 2) segmentation and, of course, 3) extraction of drainage networks from DEM images.

A medialness measure essentially assigns to each point within an object the distance to its boundary according to a given metric. The farthest points are those in the middle of the object. Therefore, we can view the medial axis as

the ridges of the medialness, which is in turn the degree of symmetry around each point. Although this is one approach to define the medial axis or skeleton of binary objects, it is desirable to extend this concept to grey-level objects, that is, those whose boundaries are unknown. The intensity axis of symmetry proposed by Gauch and Pizer [6] goes in this way. But also creases (that is, ridges for bright objects and valleys for dark ones) and creaseness measures like the level curves curvature have been proposed as a reliable approximation to the medial axis and medialness, respectively. Figure 1 shows an example. This is the approach taken in a number of applications like fingerprint analysis [9, 18], road delineation in aerial images [20, 28], hand-written OCR [32, 12] and medical image analysis [1, 26, 19].

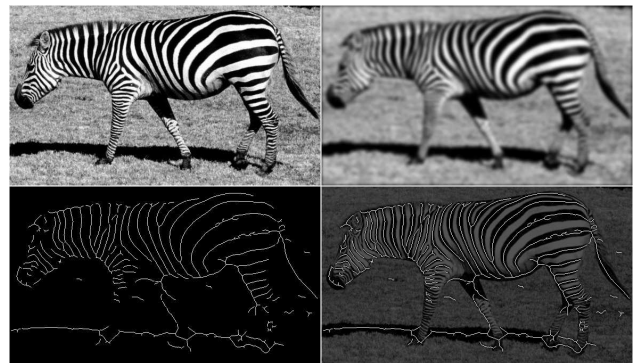


**Figure 1.** (a) black fringes of the zebra are valleys, white fringes are ridges; (b) Gaussian smoothing of a); (c) 'valleys' from the zebra, which have been extracted simply by thresholding the level curves curvature and discarding short segments; (d) c) over a).

Segmentation has also been approached through crest lines, though it is no wonder given the huge number of proposed methods along the years. Contours can be assimilated to ridges of the (regularized) gradient. One of the main concerns of segmentation techniques is to assure closed contours, in order to avoid any edge linking postprocess. For this reason, most often they resort to a type of ridges which

we will name ‘separatrices’ (section 2). In particular, the watershed transform created by the mathematical morphology school [34]. This, and other separatrix schemes partition the image into basins and hills, which are the sought regions. Their main drawback is the image oversegmentation due to irrelevant critical points to which these methods are very sensitive. Hence, computation of separatrices is often preceded by a filtering phase in order to get rid of such points, considered a kind of noise. Figure 2 shows an example, in which a ridge and a valley line are taken as markers of a watershed transform, being markers another strategy to avoid fragmentation.

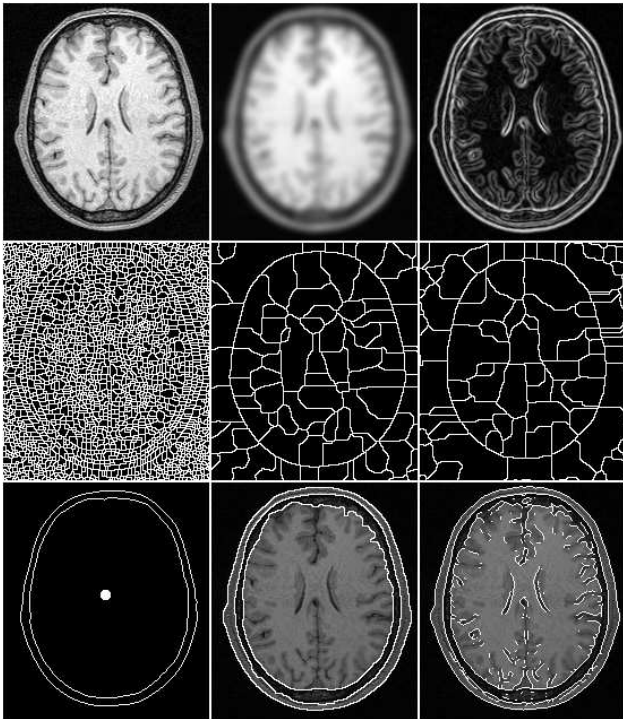


Figure 2. (a) MR slice; (b) Gaussian smoothing; (c) gradient magnitude of b); (d) watersheds of the gradient magnitude; (e) watersheds of the smoothed image; (f) watercourses of the smoothed image; (g) markers: largest creases by thresholding  $\kappa$  plus an interior point of the brain, and the image border; (h) boundaries found by the watershed transform using the markers; (i) creases obtained by thresholding  $\kappa$  of c).

We can not forget the application domain the closest to the adopted landscape image model, namely, the analysis of DEMs. It usually means the extraction of the drainage pattern (figure 3). Many studies in geomorphology and hydrology require the delineation of stream channels and divide line networks. For instance, the shape of the drainage pattern gives a clue on the type of soil composing the terrain, as it determines the way erosion acts. Methods for drainage pattern delineation consists in the simulation of rain water

fall, that is, to compute the accumulation of water at each point if we suppose it follows the steepest descent path.

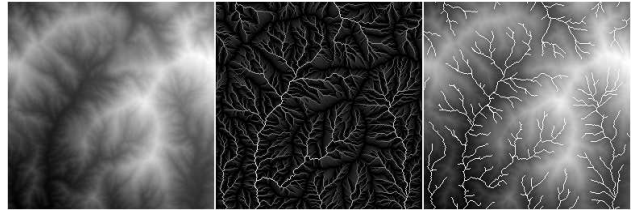


Figure 3. (a) sampled DEM; (b) logarithmic display of its accumulation array; (c) main drainage channels.

In this paper we focus on ridge and valley lines in two-dimensional images, and their extension to three dimensions. These two dual geometric entities have comparatively received little attention from the computer vision community with regard other ones like contours or, to a lesser extent, corners and junctions. And in spite of its proven utility. We believe this is due to several reasons.

Firstly, the concepts of ridge and valley are not simple, clearly distinct and unambiguous. We can loosely say that valley lines are the places where rain water in a terrain gathers to run downhill, and ridge lines are the valley lines of the relief turned upside-down. But then, could we distinguish them from the profusion of terms in English (alike in French and Spanish) to refer to similar but not identical concepts, like ‘crease’, ‘crest’, ‘divide line’ or ‘watershed’ for ridge, and ‘watercourse’, ‘creek’, ‘groove’, ‘ravine’, ‘trough’ or ‘thalweg’ for valley ?

Secondly, in an attempt to precisely define what ridge and valley lines are, a number of mathematical characterizations have been proposed since mid XIX century, and most of them are not completely equivalent. Some of them are even clearly distinct.

Finally, several of these definitions have been approximated by different operators or algorithms in order to be applied to digital images. Thus, for instance, we can find in the literature several attempts to compute the extrema of curvature of the relief’s level curves, a characterization that we will call the vertex condition.

This article aims at reviewing and establish a coherent taxonomy of ridge and valley mathematical characterizations (section 2). In particular, we intend to express each one in a common notation, thus stressing their differences and similarities. Section 3 shows the application of a creaseness measure based on the vertex condition in three problems on image registration, the domain in which we have been working in the last few years. Finally, we summarize the conclusions in section 4.

## 2. A taxonomy

In hydrology, the word *runoff* refers to the flow of water over the Earth's surface. The flowing water seeks the easiest downhill route, which is the one that follows the *steepest slope*. These routes of steepest slope are called *slopelines* or *flowlines*, and constitute the integral curves of the relief's gradient vector field. Therefore, the family of slopelines is perpendicular to that of *level curves*, which are the lines of points at equal height that appear in cartographic maps.

Since water goes downhill following the steepest descent paths, each channel can be represented by the special slope-line along which the water coming from other slopelines gathers. The set of all these special slopelines constitutes the drainage pattern.

The historical attempts to mathematically characterize the drainage pattern of a landscape gave rise to other interesting geometric entities that later have been adopted and generalized in computer vision. We have classified them as *local*, *multilocal* and *global*, according to the region of influence induced by the nature of each definition. Given the function  $L : \Omega \subset \mathbb{R}^d \rightarrow \Gamma \subset \mathbb{R}$  we have:

- **Local definitions.** At each point  $\mathbf{x} \in \Omega$ , they make a local test based on the local jet  $J_n[L](\mathbf{x}) = \{\partial^j L / \partial \alpha_1 \cdots \partial \alpha_j\}_{j=0}^n$ , that tries to identify the local anisotropy of the relief. We will use the term *creases* for both the ridge and valley structures defined by such a local test. Some of these tests provide a degree of ridgeness or valleyyness (creaseness) instead of classifying the point as lying on a crease or not.
- **Multilocal definitions.** At each point  $\mathbf{x} \in \Omega$ , these methods depend not only on  $J_n[L](\mathbf{x})$  but also on the jets at points in a region of influence. This region can be a fixed neighborhood for each  $\mathbf{x}$ , or be determined by the image geometry. This last case includes drainage patterns since the runoff in a zone does not depend on the runoff of zones arbitrarily far away.
- **Global definitions.** When the classification of a point  $\mathbf{x} \in \Omega$  as ridge/valley depends on image features at an arbitrary distance from  $\mathbf{x}$ , we consider the method to be global. In this class we include algorithms that divide the space  $\Omega$  into districts by special lines called *separatrices*. The well known watershed transform produces a type of separatrices.

## 2.1. Creases

### 2.1.1 The Saint-Venant/Haralick's Condition

One of the first works on the characterization of drainage lines dates back to 1852 and is credited to Saint-Venant<sup>1</sup> who classified a point as being on a *fatte* (ridge) or on a *talweg* (valley) if it was a locus of minimum slope along a level curve of the relief. Saint-Venant's definition can be tested locally and it can be written [29, 2] in compact tensorial form as:

$$L_{\mathbf{v}\mathbf{w}} = 0 \quad \text{and} \quad |L_{\mathbf{v}\mathbf{w}}| < |L_{\mathbf{v}\mathbf{v}}|, \quad (1)$$

where  $L_{\mathbf{v}\mathbf{v}} < 0$  means ridge and  $L_{\mathbf{v}\mathbf{v}} > 0$  valley. According to the tensorial notation used in [30],  $\mathbf{w}$  denotes the gradient direction,  $\mathbf{v}$  the orthogonal direction to the gradient and  $L_{\mathbf{u}}$  the derivative of  $L$  in the direction of vector  $\mathbf{u}$ .

Saint-Venant's condition fails to detect the special slope-lines that form the landscape's drainage pattern. The curvature of the slopelines can be defined as:

$$\mu = -L_{\mathbf{v}\mathbf{w}}/L_{\mathbf{w}} \quad , \quad (2)$$

Therefore,  $L_{\mathbf{v}\mathbf{w}} = 0$  along a slopeline would imply that it is a straight line, which means that valley lines should be planar curves confined in vertical planes, clearly in conflict with reality.

As it is noted in [10], Saint-Venant's condition has been later reformulated by Haralick [8] as loci of extremal height of  $L$  in the direction along which  $L$  reaches the greatest magnitude of its second order directional derivative. Let  $\lambda_1$  and  $\lambda_2$  be the eigenvalues of  $\nabla\nabla L$ , with  $|\lambda_1| \geq |\lambda_2|$ , and  $\mathbf{v}_1$  and  $\mathbf{v}_2$  their corresponding eigenvectors. Then,  $\mathbf{v}_1$  and  $\mathbf{v}_2$  are the directions in which the second directional derivative of  $L$  is extremized and  $\lambda_1, \lambda_2$  being the values of each extremum. Therefore, following Haralick, an equivalent definition is :

$$L_{\mathbf{w}\mathbf{v}_1} = 0 \quad , \quad (3)$$

where  $\lambda_1 < 0$  means ridge and  $\lambda_1 > 0$  valley. When the Haralick condition (3) holds, we obviously have  $\mathbf{v}_1 = \mathbf{v}$  and  $\lambda_1 = L_{\mathbf{v}\mathbf{v}}$ .

### 2.1.2 The vertex condition

Another typical local crease detector that has been claimed to delineate the drainage patterns [11] looks for extrema of the curvature of the relief's level curves. The curvature of the level curves can be defined in terms of the landscape derivatives as:

$$\kappa = -L_{\mathbf{v}\mathbf{v}}/L_{\mathbf{w}} \quad , \quad (4)$$

<sup>1</sup>References to historical papers by Saint-Venant, Cayley, Maxwell, Rothe and others can be found in [16]

where, the sign of  $\kappa$  classifies the surface as convex ( $\kappa > 0$ ) or concave ( $\kappa < 0$ ) with respect to the vertical axis. In [6, 4, 31] the crease condition for a 2D image is formulated as:

$$\nabla\kappa \cdot \mathbf{v} = 0, \quad (5)$$

where  $\mathbf{v}^t \cdot \nabla\nabla\kappa \cdot \mathbf{v} < 0$  and  $\kappa > 0$  means ridge, and  $\mathbf{v}^t \cdot \nabla\nabla\kappa \cdot \mathbf{v} > 0$  and  $\kappa < 0$  means valley. These maxima in magnitude of the curvature are connected from one level to the next, forming a subset of the so-called *vertex curves* [6] or *extremal curvature curves* [31].

Looking at the level curves of a map, it seems intuitively a reasonable assumption that valley vertex curves are the loci where water gathers. However, intuition drive us to an erroneous conclusion since vertex curves are not necessarily slopelines and, therefore, there exist non-generic situations where water does not accumulate along a valley vertex curve. Examples are the oblique gutter and the curved gutter in [10].

### 2.1.3 Mean curvature

Related to the principal curvatures of a surface we have the mean curvature  $\kappa_m$ , which is the arithmetic mean of all the principal curvatures. In [22] maxima of  $|\kappa_m|$  in any direction were classified as crease points in the context of range images. In [4], 1D crease points were identified as local extrema of the mean curvature  $\kappa_m$  of a hypersurface, that is, points where  $\nabla\kappa_m = 0$ .

### 2.1.4 Creaseness measures

For some applications we may be more interested in a creaseness measure rather than in a ridge/valley classification of the pixels. If the Haralick condition (3) holds then  $\lambda_1 = L_{\mathbf{v}\mathbf{v}}$ . Therefore,  $|L_{\mathbf{v}\mathbf{v}}|$  can be taken as a creaseness measure under the rationale that if  $L_{\mathbf{v}\mathbf{v}}$  is high, then there are more chances that the second directional derivative along the direction  $\mathbf{v}$  is the highest in magnitude. The vertex condition ‘maxima in magnitude of the relief’s level curve curvature’ is thus converted into ‘high values in magnitude of the relief’s level curve curvature’. According to (4)  $L_{\mathbf{v}\mathbf{v}}$  can be considered as the measure  $\kappa$  weighted by the gradient magnitude in order to nullify its response at isotropic regions. However, this is a trade-off since along anisotropic structures  $L_{\mathbf{w}}$  is also lower on the center of a ridge/valley region than it is on its boundary. In [33, 17], the family of operators  $L_{\mathbf{v}\mathbf{v}}L_{\mathbf{w}}^\alpha$ ,  $-1 \leq \alpha \leq 0$  was defined, where  $\alpha$  controls the trade-off between  $L_{\mathbf{v}\mathbf{v}}$  and  $\kappa$ .

The same authors went to 3D not by a direct tensorial extension of  $L_{\mathbf{v}\mathbf{v}}$  or  $\kappa$ , but by means of the operators  $L_{\mathbf{p}\mathbf{p}}$  and  $L_{\mathbf{q}\mathbf{q}}$ . If  $\mathcal{S}_{L(\mathbf{x})}$  is the level surface passing through the point  $\mathbf{x}$  and  $T\mathcal{S}_{L(\mathbf{x})}$  is its tangent plane, then we denote by  $\mathbf{p}, \mathbf{q} \in T\mathcal{S}_{L(\mathbf{x})}$  the principal directions of  $\mathcal{S}_{L(\mathbf{x})}$ ,  $\mathbf{q}$  being

the direction corresponding to the maximum principal curvature and  $\mathbf{p}$  corresponding to the minimum principal curvature.

## 2.2. Separatrices

After Saint-Venant, other attempts at characterizing drainage lines were based in the work of Cayley dated in 1859. He considered local elevation maxima, minima and saddle points: *summits*, *immits* and *knots*, respectively, in his terminology. Cayley observed that in general the level curves around a knot consist of a family of concentric hyperbolas and stated that there are only two slopelines ‘crossing’ the knot, those intersecting each other at right angles. He termed these slopelines *ridge* and *course lines*. For the ridge line the knot is a point of minimum elevation, for the course line it is a point of maximum elevation. The ridges are considered to end in a summit. Thus, a ridge line is a slopline going from one summit to another through a single knot. Similarly, course lines are considered slopelines going from an immit to another through a single knot or reaching the sea level instead of an immit.

In 1870 Maxwell continued the work of Cayley. He stated that through each point passes a slopline which ends at a certain maximum and begins at a certain minimum. Then, he defined the *basins* or *dales*, as districts whose slopelines come from the same minimum, and *hills* as districts whose slopelines run to the same maximum. In this way the landscape may be independently divided into basins and hills. Watersheds were then defined as slopelines separating basins, and watercourses as slopelines separating hills. In this way watersheds are the only slopelines which do not reach a minimum, watercourses the only slopelines that do not reach a maximum.

Nackman [21] formulated the work of Maxwell in terms of the so-called *slope districts*. A slope district is defined as the overlapping region between a basin and a hill. Rosin [25] approximates a discrete image by piecewise continuous patches. This was done by interpolating an extra point in the center of every four neighbor pixels, having as grey value the average of them. The original and interpolated pixels were then triangulated to obtain a continuous surface. Next, maxima, minima and saddles are found. After, slopelines are grown uphill and downhill from saddles to terminate at maxima and minima, respectively. A similar approach was presented by Griffin [7] who directly triangulated the pixels without interpolating a middle center point. In both cases, due to the discrete nature of images, rare situations appear making difficult the partition of the image into the slope districts of Nackman. The mathematical morphology school has proposed several algorithmic definitions of watersheds [34] in digital spaces. The most efficient algorithm is based on an immersion process analogy, in which the flooding of

water in the image is efficiently simulated by using hierarchical queues.

### 2.3. Drainage patterns

According to Koenderink and van Doorn [10] the proper mathematical characterization of the drainage pattern of a terrain goes back to 1915 and is due to R. Rothe. He stated that the lines sketching the drainage pattern of a surface must be sloopelines, a restriction that cannot be guaranteed by local conditions. Rothe identified valleys as (parts of) sloopelines where other sloopelines converge and eventually join them in a minimum (maybe at infinity) to form a stream.

Mathematically, these special sloopelines are singular solutions of the ordinary differential equation defining the sloopeline family  $\varphi = \mathbf{v} \cdot d\mathbf{x} = 0$  where  $d\mathbf{x} = (dx, dy)$ . It is well-known that it is not an exact form since it is not closed. This in turn means that we can express it as  $\varphi = \theta d\omega$ , where  $\theta$  and  $\omega$  are not uniquely defined functions. After a rather non-trivial geometric reasoning [10] the condition to identify the special sloopelines was found to be:

$$\theta L_{\mathbf{v}\mathbf{w}} = 0, \quad (6)$$

where  $L_{\mathbf{v}\mathbf{w}} = 0$  is the Saint-Venant's condition, which is a wrong one, and  $\theta = 0$  is Rothe's proposal. However, somehow the discussion about which is the right characterization of these special sloopelines still remains [24].

Researchers working with real topographic data (DEMs) extract drainage patterns not through literal implementation of Rothe's characterization but by a simulation process. The runoff simulation basically consists of measuring the number of drops of water arriving to each pixel. A drop of water starts at a pixel and goes downhill by following the gradient orientation until a minimum or the image border is reached. The drop increases the count of the pixels that visits along its way. Rothe's special sloopelines in the continuous domain are thus found (maybe unconsciously) as those segments which exhibit a higher overlapping of discrete sloopelines.

The automatic procedures that extract drainage patterns from square sampled DEMs can be divided in two main groups attending to the routing strategy they use, that is, how water is propagated from a given pixel to simulate the runoff:

- single flow algorithms: the water in a given pixel is drained to only one of its neighbors [5, 27].
- multiple flow algorithms: the water in a given pixel is distributed among several of its neighbors [23, 3].

Both types of algorithms have as main problem the presence of pits and flat areas since runoff stops at these landscape features. The main disadvantage of single flow algorithms is their inability to accommodate divergent flow,

which can produce errors in convex hills. On the other hand, they are able to accommodate quite well convergent flow. The main disadvantage of multiple flow algorithms is precisely that they spread the water even in convergent areas and hence the concentration along the channels is less salient.

## 3. Three image registration applications

In this section we try to illustrate the usefulness of ridge and valley lines in the context of a class of applications, namely, image registration. More specifically, we have developed a new creaseness operator to detect these structures, which is based on the vertex condition, that is, the curvature of the level curves (in general,  $d - 1$  sets for  $d$ -dimensional images) [16, 15]. This operator, called ST-MLSEC for "structure tensor multilocal level set extrinsic curvature", is employed to detect ridge and valley lines. They are later input as landmarks into a hierarchical search process whose output is the value of the rigid transform parameters that best align the two sets of landmarks in the sense of maximize correlation. ST-MLSEC overcomes two problems which suffer other crease measures based on the curvature like  $L_{\mathbf{v}\mathbf{v}}$  or direct estimations of curvature  $\kappa$ : discontinuities around extrema and saddle points, and unbounded response. Besides, it yields a clean and robust response, its degree of sensitivity can be adjusted and the localization is quite precise. For these reasons, we have found it to be very suitable in the following registration problems.

### 3.1. CT and MRI volumes

The registration of CT and MRI brain volumes of a same subject allows to combine partially complementary information. While CT depicts the bone accurately, MRI differentiates soft tissues much better. The problem of fusing these two types of images appears because the patient head is not exactly in the same position and orientation with respect to the CT and MRI scanners, hence a geometric transform or mapping must be found that aligns the two volumes. Since the skull does not deform, we can assume that the transform relating the two coordinate systems is rigid, that is, a 3D translation, scaling and rotation. While scaling parameters can be deduced from the image resolution, the rest can not. To do so, the skull is taken as anatomical landmark for registration. We observe that the skull forms a 3D ridge in the CT and a valley in the MRI images. Our method is quite similarly to that of van den Elsen [33], except that they employ  $L_{\mathbf{p}\mathbf{p}}$ ,  $L_{\mathbf{q}\mathbf{q}}$  and their search strategy is different and much slower than ours. Figure 4 and 5 show two examples. Reference [13] has the details and provides quantitative assessment. It is interesting to note that results are comparable and better in some situations than those of

registration by maximization of the mutual information, a kind of method of reference in the medical image registration field.

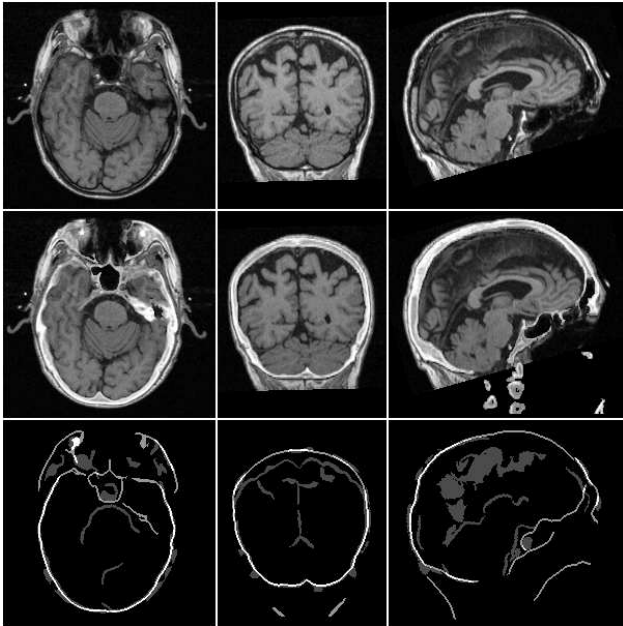


Figure 4. Top row: MRI registered to CT. Middle: CT bone overlapped to registered MRI. Bottom: CT ridges (white) over MRI valleys (grey)

### 3.2. Retinographies

Retinal images, which show the vascular tree of the eye, are an important mean to assess the condition of the retina. For a number of diseases, it is convenient to track the evolution of vessels through the years in temporal series. Also, studies are performed to quantify blood flow velocity along vessels from an animated sequence. In all cases, it is necessary to register the images before performing a point-wise comparison, because the position and orientation of the eye can change. There are several retinal imaging modalities. Retinographies taken by an ophtalmoscope under natural light are called “green images”, as a green filter is put in front of the lens to enhance the visibility of vessels. Fluoresceinic angiographies sense the fluorescence emitted from vessels after the injection of a contrast dye. SLO stands for scanning laser ophtalmoscopy and is a novel angiographic technique which registers how vessels are filled by the blood flow in order to compute the time delay at points of interest. The central idea is that vessels can be taken as landmarks. Moreover, they are thin and elongated bright objects over a darker background. Thus, they can be thought as creases (ridges) and reliably delineated by the creaseness measure we propose. Figure 6 shows the registration of a pair of SLO

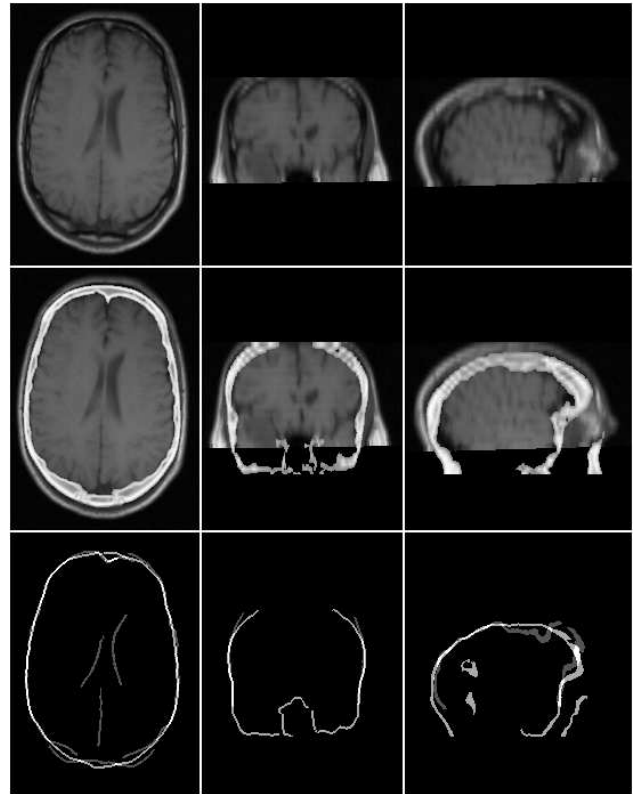


Figure 5. same as fig. 4 for a T1 weighted and lower resolution MRI

frames. Details on the mapping parameters and the search method are explained in [14].

### 3.3. Mosaicing

This last example deals with the registration of pictures for mosaicing. Concretely, they are images of the famous Michelangelo’s statue “La Pietá”. Conventional pictures of many small patches of the surface are taken to be later superimposed to a three-dimensional model of the statue (texture mapping). The shadowing due to lighting conditions creates ridge and valley lines that, even though they do not correspond to the actual ridges and valleys of the 3D model, can be used as landmarks for registration. Figure 7 shows the result for two adjacent patches.

## 4. Summary

The attempt of mathematically characterize the drainage pattern gave rise to several proposals, some of them clearly wrong. During the second half of the XIX century there was debate about what was the correct characterization. Computer vision seems to have continued this controversy, at least in the sense of a variety of algorithms and operators

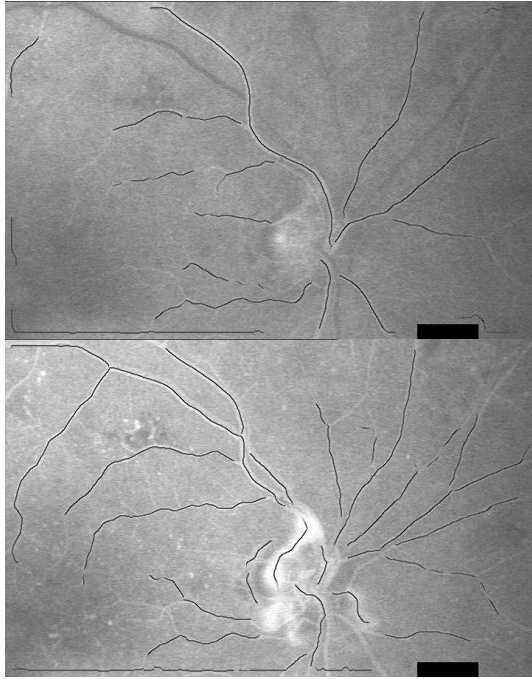


Figure 6. (a) and (b) : two SLO frames several seconds apart and their ridges; (c) ridge registration; (d) frame difference

to extract ridge and valley lines. Our point is that whether a definition fails to find the actual drainage pattern or not, it really does not matter since most of the times we merely want to sketch the medial lines in images other than DEMs. Therefore, we can choose between the hydrologic and the morphologic viewpoint attending to their own merits with

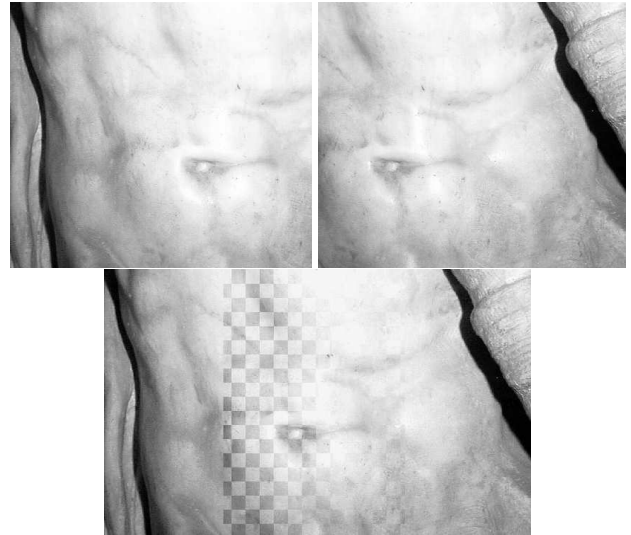


Figure 7. (a) two patches (b) fusion of the registered patches, the checkerboard appears because we visualize a small square of each image alternatively. Original images courtesy of IBM Corp.

regard to the specific application at hand.

Also, we have shown that crease lines, a characterization of ridge and valley lines based on the curvature of level sets, are suitable to register very different types of images. The three examples have in common that the landmarks used to register the images are precisely lines of ridge and valley, which we are able to detect quite reliably. This can be so even for non-medical images, like in the statue pictures or remote sensing images.

## Acknowledgments

This research has been funded by CICYT grants TIC97-1134-C02-02 and TAP98-0618. CT and MRI volumes were kindly provided by Dr. van den Elsen from Utrecht University and Dr. J.M. Fitzpatrick from Vanderbilt University. Thanks also to Cástor Perez Mariño from Universidade da Coruña for providing the SLO example.

## References

- [1] N. Armande, O. Monga, and P. Montesinos. Thin nets extraction in medical images. In Y. Bizais, editor, *Proc. Int. Conf. on Information Processing in Medical Imaging*, Lecture Notes in Computer Science, pages 383–384. Springer-Verlag, 1995.
- [2] S. Chinveeraphan, R. Takamatsu, and M. Sato. Understanding of ridge-valley lines on image-intensity surfaces in scale-space. In Hlavac and Sara, editors, *Proc. Int. Conf. on Computer Analysis of Images and Patterns*, volume 970 of *Lec-*

- ture Notes in Computer Science, pages 661–667. Springer-Verlag, 1995.
- [3] J. Desmet and G. Govers. Comparison of routing algorithms for digital elevation models and their implications for predicting ephemeral gullies. *Inter. Journal of Geographical Information Systems*, 10:311–331, 1996.
  - [4] D. Eberly, R. Gardner, B. Morse, S. Pizer, and C. Scharlach. Ridges for image analysis. *Journal of Mathematical Imaging and Vision*, 4:353–373, 1994.
  - [5] J. Fairfield and P. Leymarie. Drainage networks from grid digital elevation models. *Water Resources Research*, 27:709–717, 1991.
  - [6] J. Gauch and S. Pizer. Multiresolution analysis of ridges and valleys in grey-scale images. *IEEE Trans. on Pattern Analysis and Machine Intelligence*, 15:635–646, 1993.
  - [7] L. Griffin, A. Colchester, and G. Robinson. Scale and segmentation of grey-level images using maximum gradient paths. *Image and Vision Computing*, 10:389–402, 1992.
  - [8] R. Haralick. Ridges and valleys on digital images. *Computer Vision Graphics and Image Processing*, 22:28–38, 1983.
  - [9] A. Jain, L. Hong, and R. Bolle. On-line fingerprint verification. *IEEE Trans. Pattern Analysis and Machine Intelligence*, 19:302–313, 1997.
  - [10] J. Koenderink and A. van Doorn. Local features of smooth shapes: ridges and courses. In *Geometric Methods in Computer Vision II*, volume 2031, pages 2–13. SPIE, 1993.
  - [11] I. Kweon and T. Kanade. Extracting topographic terrain features from elevation maps. *CVGIP: Image Understanding*, 59:171–182, 1994.
  - [12] S. Lee and Y. Joon. Direct extraction of features for gray scale character recognition. *IEEE Trans. Pattern Analysis and Machine Intelligence*, 17:724–729, 1995.
  - [13] D. Lloret, A. López, J. Serrat, and J. Villanueva. Creaseness-based CT and MR registration: comparison with the mutual information method. *Journal of Electronic Imaging*, 8(3):255–262, 1999.
  - [14] D. Lloret, J. Serrat, A. López, and J. Villanueva. Retinal image registration using creases as anatomical landmarks. In J. V. A. Sanfeliu, editor, *Proc. Int. Conf. on Pattern Recognition*. IAPR, IEEE Computer Society, September 2000.
  - [15] A. López, D. Lloret, J. Serrat, and J. Villanueva. Multi-local creaseness based on the level set extrinsic curvature. *Computer Vision and Image Understanding*, 2(77):111–144, 2000.
  - [16] A. López, F. Lumbreras, J. Serrat, and J. Villanueva. Evaluation of methods for ridge and valley detection. *IEEE Pattern Analysis and Machine Intelligence*, 21(4):327–335, 1999.
  - [17] J. Maintz, P. van den Elsen, and M. Viergever. Evaluation of ridge seeking operators for multimodality medical image matching. *IEEE Trans. on Pattern Analysis and Machine Intelligence*, 18:353–365, 1996.
  - [18] D. Maio and D. Maltoni. Direct gray-scale minutiae detection in fingerprints. *IEEE Trans. Pattern Analysis and Machine Intelligence*, 19:27–39, 1997.
  - [19] A. Manceaux-Demiau, J. Mangin, J. Regis, O. Pizzato, and V. Frouin. Differential features of cortical folds. In J. Trocaz, E. Grimson, and R. Mosges, editors, *Proc. 1st Joint Conf. on Computer Vision, Virtual Reality and Robotics in Medicine and Medical Robotics and Computed-Assisted Surgery*, volume 1205 of *Lecture Notes in Computer Science*, pages 439–448. Springer-Verlag, 1997.
  - [20] O. Monga, N. Armande, and P. Montesinos. Thin nets and crest lines: Application to satellite data and medical images. In *Proc. IEEE Inter. Conf. on Image Processing*, pages 468–471. IEEE Computer Society Press, 1995.
  - [21] L. Nackman. Two-dimensional critical point configuration graphs. *IEEE Trans. on Pattern Analysis and Machine Intelligence*, 6:442–450, 1984.
  - [22] S. Pankanti, C. Dorai, and A. Jain. Robust feature detection for 3D object recognition and matching. In *Geometric Methods in Computer Vision II*, volume 2031, pages 366–377. SPIE, 1993.
  - [23] P. Quinn, K. Beven, P. Chevalier, and O. Planchon. The prediction of hillslope flow paths for distributed hydrological modelling using digital terrain models. *Hydrological Processes*, 5:59–79, 1991.
  - [24] J. Rieger. Topographical properties of generic images. *International Journal of Computer Vision*, 23:79–92, 1997.
  - [25] P. Rosin, A. Colchester, and D. Hawkes. Early image representation using regions defined by maximum gradient paths between singular points. *Pattern Recognition*, 25:695–711, 1992.
  - [26] Y. Sato, S. Nakajima, N. Shiraga, H. Atsumi, S. Yoshida, T. Koller, G. Gerig, and R. Kikinis. Three-dimensional multi-scale line filter for segmentation and visualization of curvilinear structures in medical images. *Medical Image Analysis*, 2:143–168, 1998.
  - [27] P. Soille and M. Ansoult. Automated basin delineation from digital elevation models using mathematical morphology. *Signal Processing*, 20:171–182, 1990.
  - [28] C. Steger. Extracting curvilinear structures: a differential geometric approach. In B. Buxton and R. Cipolla, editors, *Proc. 4th Euro. Conf. on Computer Vision*, volume 1064 of *Lecture Notes in Computer Science*, pages 630–641. Springer-Verlag, 1996.
  - [29] B. Ter Haar Romeny, editor. *Geometry-Driven Diffusion in Computer Vision*. Kluwer Academic Publishers, 1994.
  - [30] B. ter Haar Romeny and L. Florack. A multiscale geometric model of human vision. In W. Hendee and P. Well, editors, *The Perception of Visual Information*, pages 73–114. Springer-Verlag, 1993.
  - [31] J. Thirion and A. Gourdon. Computing the differential characteristics of iso-intensity surfaces. *Computer Vision and Image Understanding*, 61:190–202, 1995.
  - [32] O. Trier, T. Taxt, and A. Jain. Recognition of digits in hydrographic maps: Binary versus topographic analysis. *IEEE Trans. on Pattern Analysis and Machine Intelligence*, 19:399–404, 1997.
  - [33] P. van den Elsen, J. Maintz, E.-J. Pol, and M. Viergever. Automatic registration of CT and MR brain images using correlation of geometrical features. *IEEE Trans. on Medical Imaging*, 14:384–396, 1995.
  - [34] L. Vincent and P. Soille. Watersheds in digital spaces: An efficient algorithm based on immersion simulations. *IEEE Trans. Pattern Analysis and Machine Intelligence*, 13:583–598, 1991.